Lewis number and curvature effects on sound generation by premixed flame annihilation

By M. Talei†, M. J. Brear† AND E. R. Hawkes‡

A numerical and theoretical study of sound generation by planar, axisymmetric and spherically symmetric premixed laminar flame annihilation is presented in this paper. The compressible Navier-Stokes, energy, and progress-variable equations are solved using Direct Numerical Simulation (DNS) with one-step chemistry. The sound produced for these three configurations is compared for different Lewis numbers. A theory is developed in the case of unity Lewis number using the propagation velocity and consumption speed, which were identified as key parameters in the generation of sound in our previous study (Talei *et al.* 2010). The results show that by obtaining the propagation velocity of the flame from the simulations, the sound generation can be predicted accurately for unity Lewis number. Use of Markstein's linear theory leads to under-prediction of the sound radiated.

Cases involving non-unity Lewis number are then investigated. As the flames approach annihilation, either flame acceleration or deceleration is observed depending on the Lewis number, and this is shown to have a significant contribution to the sound radiated. For Lewis numbers greater than unity, the annihilation of the flame results in a local increase in consumption speed at annihilation, leading to more sound production compared with that of unity Lewis number. Lewis numbers less than unity exhibit the opposite behavior.

1. Introduction

Combustion is a significant source of noise pollution. Combustion-generated sound also plays a central role in the stability of many engineering devices such as industrial burners, gas turbines, and rockets (e.g. Lieuwen 2003; Candel *et al.* 2009). The ongoing pursuit of quieter and cleaner combustion in these devices provides a continued need for further refinements in our understanding of combustion-generated sound.

Strahle (1971) constructed a theory of combustion noise by extending Lighthill's acoustic analogy (Lighthill 1951) to combusting flows. He argued that monopolar sound sources can appear in turbulent combusting flows. Under the assumptions of low Mach number and a constant, average-mixture molecular weight, Lighthill's acoustic analogy can be simplified to an inhomogeneous wave equation with a single monopolar source term (Strahle 1978; Dowling 1992). This source term has been written in terms of time derivatives of the heat release rate or the flame volume (e.g. Strahle 1978).

One mechanism affecting the flame volume, and hence sound generation, is flame annihilation (Kidin *et al.* 1984; Candel *et al.* 2004). For example, when two flame surfaces interact the unburnt gas trapped between these surfaces is consumed, resulting in a rapid reduction in flame surface area and thus heat release. Candel *et al.* (2004) studied sound

† Department of Mechanical Engineering, University of Melbourne
‡ School of Photovoltaic and Renewable Energy Engineering/School of Mechanical and Manufacturing Engineering, University of New South Wales

generation by mutual flame annihilation and concluded that the dominant mechanism of sound generation was flame surface destruction.

Our previous work (Talei *et al.* 2010) examined sound generation by premixed, laminar flame annihilation for unity Lewis number. The main aim of this study is therefore to investigate Lewis number effects on the mechanism of sound generation in planar, axisymmetric and spherical flame annihilation. We also extend our earlier theoretical results to include the linear theory of Markstein (1964) in an attempt to close the sound generation problem. These more general theoretical results are also compared with the simulations.

2. Numerical Methods and Flow Parameters

A modified version of NTMIX (Cuenot *et al.* 1997) is used. NTmix is a high-order accurate solver with single-step chemistry. It features a 6^{th} order compact scheme for spatial derivatives, combined with a 3^{rd} order Runge-Kutta time integrator. These modifications include the ability to simulate axisymmetric and spherically symmetric geometries. Fully three-dimensional characteristic boundary conditions (Lodato *et al.* 2008) were also implemented. Further details of numerical methods are presented in our previous study (Talei *et al.* 2010). The governing equations were discretized into 3000 nodes from $\zeta = 0$ to $15L_{ref}$, where L_{ref} is the reference length and ζ is the spatial coordinate in the planar, axisymmetric and spherical cases. The laminar flame thickness δ is constant and equal to $0.1L_{ref}$. Three different Lewis numbers ($Le = 0.5$, 1 and 2) have been studied. The Prandtl number is 0.75. The temperature ratio T_b/T_u is 4 where T_u is the fresh gas temperature and T_b is the burned gas temperature for an unstretched laminar flame with unity Lewis number. The Zel'dovich number β is 8.

3. Results and discussion

3.1. *Numerical results for unity Lewis number*

We first briefly review the process of annihilation and the associated sound production for $Le = 1$, which was reported in our previous study (Talei *et al.* 2010). The middle column in Fig. 1 shows the reaction rate versus normalized distance x/δ at several instants. The flame propagates from right to left and the annihilation location is at the origin ($\zeta/\delta = 0$). It may be observed in this unity Lewis number case that the reaction-rate profile retains a similar spatial profile as the flame propagates. After the point of the peak reaction rate reaches the origin, the peak value decreases until the flame is annihilated.

Figure 1ii shows the reduced temperature $\theta = (T - T_u)/(T_b - T_u)$ versus normalized distance for several instants. The reduced temperature increases as the two preheat zones start to merge. After the extinction event, the temperature is uniform and equal to the burnt gas temperature throughout the domain.

Now consider the pressure field in Fig. 1. Before the annihilation event there is a small, hardly observable change in the pressure profile across the flame due to flame propagation. However, during the extinction event, the pressure at the origin first increases then decreases, leading to a much larger pressure pulse that propagates away from the symmetry plane in the positive x-direction. The generated pressure wave after the annihilation event for the planar case has a steady-state value that is less than the reference pressure.

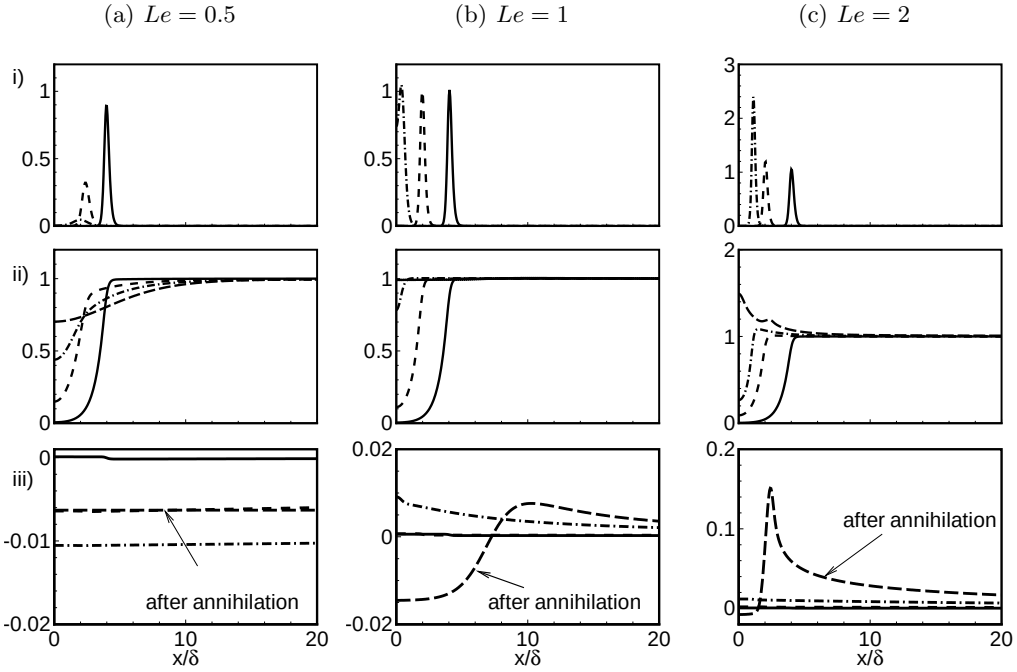

Figure 1: i) non-dimensional reaction rate $\dot{\omega}/(\dot{\omega}_{max})_\infty$, ii) reduced temperature θ, and iii) non-dimensional pressure $(p-p_{ref})/\rho_{ref}c^2_{ref}$ versus distance from the origin non-dimensionalized by flame thickness δ at different instants before (solid), during (dashed and dash-dot), and after (long dash) planar annihilation.

3.2. *Theory for unity Lewis number*

Our previous study (Talei *et al.* 2010) theorized that a constant propagation velocity could adequately predict the far-field steady state pressure for the planar configuration. However, assuming constant propagation velocity led to significant under prediction of sound in the far-field in the axisymmetric and spherically symmetric cases.

In this section we will relax one of the assumptions used in our previous, infinitely thin flame approximation in an attempt to partially account for finite flame-thickness effects. In our previous theory, we assumed that the flame displacement speed (i.e. the speed at which the location of the maximum heat release moves) and the flame consumption speed (i.e. the spatial integral of the reaction rate) were identical. Here we relax this assumption, which will be shown to lead to improved results.

In our previous study the general solution of Lighthill's equation for flames of finite thickness, retaining only the heat release term as the source term of Lighthill's equation, was

$$p'(r,t) = \left(1-\frac{T_u}{T_b}\right)\int_0^{t-r/c_b}\int_0^{\zeta^+}\frac{\zeta\partial\dot{\omega}/\partial\tau d\zeta d\tau}{\sqrt{(t-\tau)^2-r^2/c_b^2}} \tag{3.1}$$

for the axisymmetric annihilation and

$$p'(R,t) = \left(1 - \frac{T_u}{T_b}\right) H(t - R/c_b) \frac{\int_0^{\zeta^+} \zeta^2 \partial\dot{\omega}/\partial\tau d\zeta \Big|_{\tau=t-R/c_b}}{R} \tag{3.2}$$

for spherically symmetric annihilation. The variable p' is the pressure fluctuation in the far-field, r and R are the distances from the origin in the axisymmetric and spherically symmetric cases, respectively, $\dot{\omega}$ is the reaction rate, t is the time and c is the sonic velocity. These expressions are not directly useful because of the appearance of the reaction rate and its time derivative in the integrands. Some approximation is therefore required to proceed.

In order to evaluate the integral terms in Eqs. 3.1 and 3.2, the reaction rate may be modelled by a delta function and assuming a constant consumption speed,

$$\dot{\omega} = \rho_u S_L \delta(\zeta_f(\tau) - \zeta), \tag{3.3}$$

where ρ is the density, S_L is the laminar flame speed, and ζ_f is the flame position. Substituting Eq. 3.3 into Eqs. 3.1 and 3.2, the solution of Lighthill's equation for axisymmetric and spherically symmetric annihilations may be expressed as

$$p'(r,t) = -\rho_u S_L \left(1 - \frac{T_u}{T_b}\right) \int_0^{t-r/c_b} \frac{V_f(\tau) d\tau}{\sqrt{(t-\tau)^2 - r^2/c_b^2}} \tag{3.4}$$

and

$$p'(R,t) = -2\rho_u S_L \left(1 - \frac{T_u}{T_b}\right) \zeta_f(t - R/c_b) V_f(t - R/c_b) H(t - R/c_b), \tag{3.5}$$

respectively. The variable $V_f = -d\zeta_f/d\tau$ is the propagation velocity of the flame. Note, we do not assume here that V_f equals the consumption speed.

The remaining problem is to estimate the flame displacement velocity, which may depart from the laminar burning rate as annihilation is approached. A simple relation between laminar burning velocity and curvature was proposed by Markstein (1964),

$$V_f = S_L \left(1 + n L_M/\zeta_f\right), \tag{3.6}$$

where L_M is the Markstein length and $n = 1$ for axisymmetric and $n = 2$ for spherically symmetric cases respectively. Substituting Eq. 3.6 into Eqs. 3.4 and 3.5, the pressure in the far-field may be estimated for the axisymmetric annihilation as

$$p'(r,t) = -\rho_u S_L^2 \left(1 - \frac{T_u}{T_b}\right) \int_0^{t-r/c_b} \frac{(1 + L_M/\zeta_f) d\tau}{\sqrt{(t-\tau)^2 - r^2/c_b^2}}, \tag{3.7}$$

whereas for the spherically symmetric annihilation

$$p'(R,t) = -2\rho_u S_L^2 \left(1 - \frac{T_u}{T_b}\right) (\zeta_f + 2L_M) H(\zeta_f(\tau)) \Big|_{\tau=t-R/c_b}. \tag{3.8}$$

The result for the spherically symmetric annihilation is similar to the theory proposed by Kidin *et al.* (1984), which is repeated here,

$$p'(R,t) = -2\rho_u \left(1 - \frac{T_u}{T_b}\right) S_L^2 \left(1 + \frac{2L_M}{\zeta_f}\right) \left(\frac{\zeta_f + L_M}{R}\right) H(\zeta_f(\tau)) \Big|_{\tau=t-R/c_b}. \tag{3.9}$$

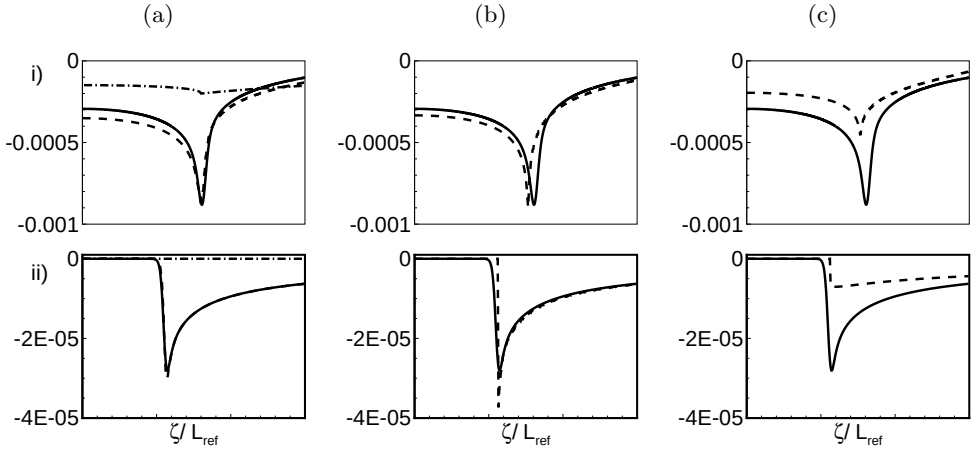

Figure 2: Comparison of DNS (solid line) and solution of Lighthill's equation (dashed line) a) using the reaction rate source term, b) obtaining propagation velocity from the simulation results, and c) using the Markstein length theory, dash-dot: analytical solution of Lighthill's equation assuming constant propagation velocity, top row; axisymmetric, bottom row; spherically symmetric.

We would obtain the same result as Kidin *et al.* (1984) if we had assumed that the displacement and consumption speeds were identical.

These different theoretical approximations are now compared. The top row of Fig. 2, which is reproduced from data of our previous study, shows the DNS result, the result from the solution of Lighthill's equation retaining only the heat-release source term and the solution assuming an infinitely thin flame that propagates at the laminar burning speed. As can be seen, retaining only the heat release source terms results in good agreement with the simulation, while the infinitely thin, constant speed result is poor. The middle column of Fig. 2 shows a numerical solution of Lighthill's equation using Eqs. 3.4 and 3.5. Here, the propagation velocity is taken directly from the simulation result by measuring the absolute displacement speed of the point of maximum reaction rate. As may be seen, for both axisymmetric and spherically symmetric annihilation events the theory can predict the sound radiated to the far field with a reasonable degree of agreement.

The right column of Fig. 2 shows a comparison of simulation results with Eqs. 3.7 and 3.8 for axisymmetric and spherically symmetric cases, respectively. The Marsktein length is 13δ for this unity Lewis number case, which is obtained from the theory developed by Clavin & Joulin (1983). As can be seen, the solution of Lighthill's equation using the Markstein length for the displacement speed captures some of the sound generation due to flame acceleration. Because the Markstein length is proportional to flame thickness, this shows that the effect of flame thickness needs to be considered.

3.3. *Non-unity Lewis number*

Figure 1i shows the reaction rate at different instants before and during the extinction event for the planar case for $Le = 0.5$, 1, and 2. It is observed that for low Lewis number, the reaction rate decreases when the flame approaches the origin. In this case, the thickness of the mass diffusion layer is larger than the thermal diffusion layer. Therefore, when the two flames approach each other the mass diffusion layers start to interact

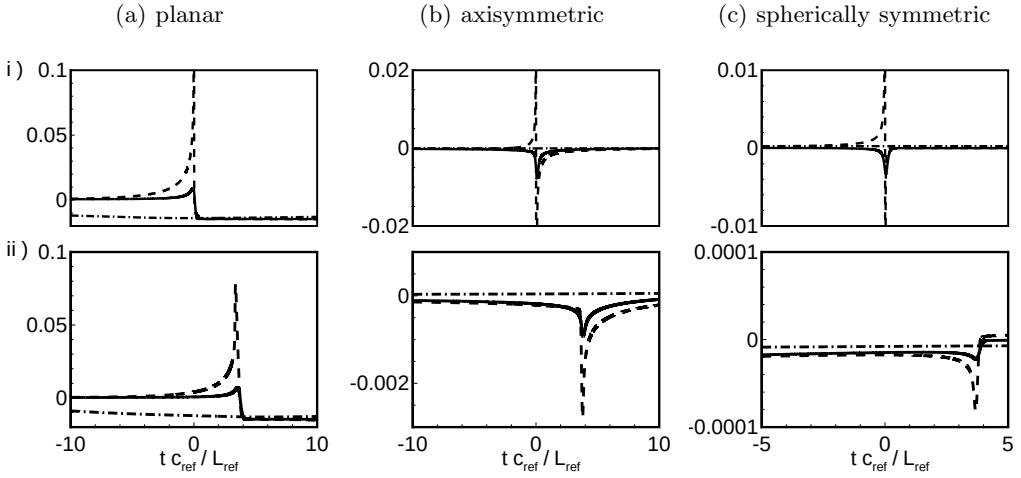

Figure 3: Relative pressure for flame annihilation from DNS i) at the symmetry axis and ii) in the far-field $x/L_{ref} = 7.5$ for different Lewis numbers: solid line, $Le = 1$; dashed, $Le = 2$; dash-dot, $Le = 0.5$.

earlier than the thermal diffusion layers, leading to the depletion of reactants before the region of greatest reaction rate reaches the symmetry plane. As a result, the extinction of the flame commences at a distance from the origin. This behavior is consistent with prior observations from planar flame extinction (e.g. Sun & Law 1998). As a result of the gradual decrease in the reaction rate the reactants burn slowly as the temperature increases (Fig. 1i and ii). The pressure shown in Fig. 1 also changes gradually over a long period of time and significantly less sound is produced compared with that in the other two cases.

The case of $Le = 2$ is shown in the rightmost column of Fig. 1. The increase in the reaction rate as the flame approaches the symmetry plane is much higher than for $Le = 1$. In this case, the reaction rate starts to increase at a greater distance from the origin, which also has a significant effect on the temperature and pressure profile before and after flame annihilation. Indeed, in this case the peak temperature exceeds the adiabatic flame temperature at some instants. The observed far-field pressure is similar to the unity Lewis number case.

Figure 3 shows a comparison of pressure versus time at two points in the domain for each of the different configurations and all three Lewis numbers. The columns from left to right correspond to the planar, axisymmetric, and spherical configurations. The Lewis numbers of $Le = 0.5$, 1, and 2 are shown. As can be seen from Fig. 3, in the case of planar flame annihilation, the high and unity Lewis number cases produce a similar steady-state far-field pressure, whereas the peak pressure is much higher for the high Lewis number. The peak pressure is due to the peak reaction rate, which was much higher in the case of the high Lewis number. In the low Lewis number case the pressure varies over a much longer period compared with the other two cases.

3.4. *Dynamics of flame annihilation*

In the theory developed in section 3.2, the propagation velocity and consumption speed were used to predict the sound generation by the annihilation event. In this section

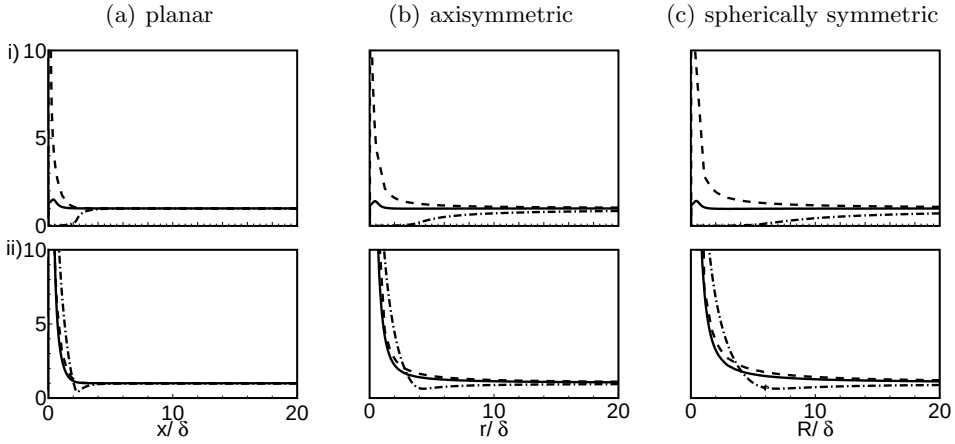

Figure 4: i) normalized consumption speed $\int_0^\infty \dot{\omega} d\zeta/\rho_u S_L$, ii) magnitude of normalized propagation velocity $|V_f|/S_L$ versus x/δ: solid line, $Le = 1$; dashed, $Le = 2$; dash-dot, $Le = 0.5$.

variation of these two parameters are investigated to assess the validity of the assumptions used.

Figure 4 shows non-dimensional consumption and propagation speeds versus non-dimensional flame position. Flame position is defined as the position of maximum reaction rate. For $Le >= 1$ the consumption speed starts to increase as the flame approaches the origin for all configurations. However, as the two flames get closer the consumption speed starts to drop and eventually tends to zero during the extinction process.

In the case of low Lewis number the consumption speed starts to decrease before the flame reaches the origin. The extinction commences at a point near the origin as the consumption speed tends to zero. The extinction at this point is not complete and there will be further reaction as the point of maximum reaction rate approaches the origin.

Figure 4ii shows the propagation velocity of the flame measured at the point of maximum reaction rate. In all cases an increase in the velocity is observed near the origin, providing justification for the earlier attempt at closing the problem using the Markstein length. As can be observed from Fig. 4i, constant consumption speed is a reasonable assumption to solve Lighthill's equation for only unity Lewis number, thus demonstrating limitations in this approximation.

4. Conclusions

This paper presents a numerical and theoretical study of sound production by flame annihilation in planar, axisymmetric, and spherically symmetric configurations. A series of Direct Numerical Simulations (DNS) using a higher order accurate solver appropriate for aeroacoustic studies was used and the effects of flame curvature and Lewis number were investigated.

In order to predict the sound generation in axisymmetric and spherically symmetric cases, a previous work by the authors was revisited by modelling the reaction rate as a constant amplitude delta function moving toward the origin. The propagation velocity of the flame was measured by tracking the point of maximum reaction rate. There was a good agreement between the simulation results and solution of Lighthill's equation using this method for unity Lewis number. In our attempt to find a more general theory,

Markstein's linear theory was then used to obtain the propagation velocity, but this was shown to lead to an under prediction of the sound radiated to the far-field.

Simulations also showed that the assumption of constant consumption speed was not always valid. For high Lewis number, an increase is observed in both the propagation velocity and consumption speed, which leads to generation of higher amplitude sound compared with unity Lewis number. In the case of low Lewis number, a decrease in the consumption speed occurred, causing flame extinction to commence before it reached the origin. This case was shown to produce significantly less sound compared with higher Lewis number cases.

The authors acknowledge the generous support of the European Centre for Research and Advanced Training in Scientific Computation (CERFACS, www.cerfacs.fr), in providing the authors with the source code for NTmix. Use of the facilities of the Center for Turbulence Research (CTR) at Stanford University during the 2010 summer program is also gratefully acknowledged.

REFERENCES

Candel, S., Durox, D., Ducruix, S., Birbaud, A. L., Noiray, N. & Schuller, T. 2009 Flame dynamics and combustion noise: progress and challenges. *Int. J. Aeroacoustics* **8** (1&2), 1–56.

Candel, S., Durox, D. & Schuller, T. 2004 Flame interactions as a source of noise and combustion instabilities. In *Collection of Technical Papers-10th AIAA/CEAS Aeroacoustics Conference*, pp. 1444–1454.

Clavin, P. & Joulin, G. 1983 Premixed flames in large scale and high intensity turbulent flow. *J. Phys. Lett.* **44** (1), 1–12.

Cuenot, B., Bedet, B. & Corjon, A. 1997 *NTMIX3D user's guide manual, Preliminary Version 1.0*.

Dowling, A. P. 1992 *Modern Methods in Analytical Acoustics*, chap. Thermoacoustic sources and instabilities, pp. 378–403. Springer.

Kidin, N., Librovicht, V., Robertst, J. & Vuillermoz, M. 1984 On sound sources in turbulent combustion. *Dynamics of flames and reactive systems* pp. 343–355.

Lieuwen, T. 2003 Modeling premixed combustion-acoustic wave interactions: A review. *J. Propulsion Power* **19** (5), 765–781.

Lighthill, M. J. 1951 On sound generation aerodynamically I. General Theory. *Proc. Roy. Soc. London* **211**, 564–587.

Lodato, G., Domingo, P. & Vervisch, L. 2008 Three-dimensional boundary conditions for direct and large-eddy simulation of compressible viscous flows. *J. Comput. Phys.* **227** (10), 5105–5143.

Markstein, G. H. 1964 *Nonsteady flame propagation*. Pergamon.

Strahle, W. C. 1971 On combustion generated noise. *J. Fluid Mech.* **49** (2), 399–414.

Strahle, W. C. 1978 Combustion noise. *Prog. Energy Combust. Sci.* **4**, 157–176.

Sun, C. J. & Law, C. K. 1998 On the consumption of fuel pockets via inwardly propagating flames. *Proceedings of the Combustion Institute* pp. 963–970.

Talei, M., Brear, M. J. & Hawkes, E. R. 2010 Sound generation by premixed flame annihilation. Submitted to the J. Fluid Mech.